

STUDY OF NATURAL CONVECTION FLOWS IN A TILTED TRAPEZOIDAL ENCLOSURE WITH ISOFLUX HEATING FROM BELOW

Hasib Uddin^{1*} and Sumon Saha²

Received: Apr 8, 2008; Revised: Sept 17, 2008; Accepted: Sept 23, 2008

Abstract

Laminar steady state natural convection in a two-dimensional symmetrical trapezoidal enclosure has been studied using a finite element method. In this investigation, the top wall is considered adiabatic, both inclined sidewalls are maintained at a constant cold temperature and an isoflux heat source is provided at the bottom surface. The pressure-velocity form of the Navier-Stokes equations and energy equation are used to represent the mass, momentum and energy conservations of the fluid medium in the enclosure. Galerkin weighted residual method of finite element formulation with triangular mesh elements is employed. The fluid investigated here is air of Prandtl number fixed at 0.7. The Rayleigh number is varied from 10^3 to 10^6 while the sidewall inclination angle is varied from -15° to 45° . The results are presented in terms of streamline and isotherm plots as well as the variation of average Nusselt number with Rayleigh number for different base wall tilt angles of 0° , 15° , and 30° . The results show that the average Nusselt number increases with the increase of Rayleigh number and the effect of the sidewall inclination angle on heat transfer is significantly reduced at higher Rayleigh number. Effects of sidewall inclination angle on convection heat transfer characteristics decrease with the increase of base wall tilt angle at higher Rayleigh number and Rayleigh number equal to 10^5 can be considered as a critical limit for the present.

Keywords: Natural convection, trapezoidal enclosure, finite element, isoflux

Introduction

Natural convection flows are particularly complex to control because they depend on several parameters among which the geometry concerned and the thermo-physical characteristics of the fluid are the most important. Natural convection in enclosures of different geometry has drawn greater attention for intensive research efforts in recent years because of its extensive application in wide range of engineering areas such as thermal insulation, geothermal reservoirs, nuclear waste management, solar collector, crystal growth and design of cooling systems

¹ Graduate Student, Department of Mechanical Engineering, University of Illinois at Urbana-Champaign, 1206, W Green St. Urbana-61801, IL, USA. E-mail: hasib_uddin@hotmail.com

² Department of Mechanical Engineering, Bangladesh University of Engineering & Technology (BUET), Dhaka-1000, Bangladesh. E-mail: sumonsaha@me.buet.ac.bd

* Corresponding author

for various electronic equipments. The enclosures phenomena can loosely be organized into two large classes (Bejan, 1984); heated from side and heated from below. The study of both flow classes is also relevant to our understanding of natural circulation in the atmosphere, the hydrosphere, and the molten core of the earth. The present investigation concentrates attention on isoflux heating from below, which mainly focuses the application of many practical transport devices such as commercially refrigerating cavities, furnaces, electronics cooling, processing equipments and others.

Actual enclosures occurring in practice often have the shapes differing from rectangular cover. Thus, various channels of constructions, panels of electronic equipment and solar energy collectors are of nonrectangular form. Moreover, a smaller number of previous studies have considered the trapezoidal geometry, which is encountered in several practical applications, such as attic spaces in buildings, greenhouses or sun drying of crops. Solution of this type of problem is not simple to obtain because of the sloping walls. In general, the mesh nodes do not lie along the sloping walls and consequently from a program-using and computational point of view, the effort required for determining the flow characteristics increases significantly.

Several geometrical configurations, more or less complex, have been examined under theoretical, numerical or experimental approaches. Nithyadevi *et al.* (2007) had investigated natural convection in rectangular cavity with partially active side walls. Heat transfer experiments in triangular enclosures were first reported by Flack *et al.* (1980). Effect of non-uniform heat flux on convection heat transfer in trapezoidal channel was experimentally studied by Remley *et al.* (2001). Kumar (2004) experimentally investigated natural convective heat transfer in trapezoidal enclosure. He focused on the performance of a box type solar cooker and evaluated the natural convective heat transfer coefficient. Ganzarolli and Milanez (1995) performed numerical study of steady natural convection in rectangular enclosures heated from below and symmetrically cooled from the sides. The size of the cavity was varied from square to shallow. Natural convec-

tion in tilted parallelepipedic cavities for large Rayleigh numbers was studied numerically and experimentally by Bairy *et al.* (2007). The majority of researches involving convection study is restricted to the cases of simple geometry like rectangular, square, cylindrical and spherical cavities. But the configurations of actual containers occurring in practice are often far from being simple. Research works on natural convection dealing with trapezoidal porous enclosures were reported by Baytas and Pop (2001) while Kumar and Kumar (2004) carried out parallel computation for various values of flow and geometric parameters both under Darcian and non-Darcian assumptions on the porous model. The heat and mass transfer by free convection in a trapezoidal enclosure heated by its lower base and cooled by its inclined upper side was studied by Boussaid *et al.* (1999). They solved the momentum, energy and mass equations by finite volume method and observed the influences of the geometrical parameters too. Kuyper and Hoogendoorn (1995) investigated laminar natural convection flow in trapezoidal enclosures to study the influence of the inclination angle on the flow and also the dependence of the average Nusselt number on the Rayleigh number. Iyican and Bayazitoglu (1980); McQuain *et al.* (1994); Van der Eyden *et al.* (1998); Reynolds *et al.* (2004); Papanicolaou and Belessiotis (2005) and several other researchers had been made several attempts to understand the basic heat transfer and fluid flow characteristics inside a trapezoidal cavity. The work similar to the current one was done by Natarajan *et al.* (2008). They considered a regular trapezoidal enclosure and maintained 30° angle of inclination of the sidewalls and investigated in detail natural convection flows with uniform and non-uniform heating of the bottom wall. They used penalty finite element method to obtain smooth solutions in terms of stream functions and isotherm contours. For convection dominant heat transfer mode, in the case of uniform heating at Rayleigh number, $Ra = 10^5$, the heat transfer rate gradually decreased from the left of the bottom wall and attained minimum at the center of the bottom wall and increased at the right. They found that the non-uniform heating exhibited greater heat

transfer at the center of the bottom wall than with uniform heating case for all Rayleigh number regimes. They also showed that for $Pr = 0.7$ and $Ra = 10^5$, the average Nusselt number during uniform heating from below was greater than that for non-uniform heating. As expected, the trend was increasing for both cases with the increase of Rayleigh number.

The current investigation demonstrates the effects of natural convection in a regular trapezoidal enclosure having isoflux heat source, q at the bottom wall under different base wall tilt angles. The inclined sidewalls are cooled by means of constant temperature (T_c) bath and the top wall is well insulated. No previous work has been found considering isoflux heating from below in the present physical model. The Galerkin finite element method (Reddy, 1993) has been used to obtain the velocity components and temperature of the working fluid. Parametric studies are carried out for $Ra = 10^3, 10^4, 10^5, 10^6$ and $Pr = 0.7$. Afterwards, the angle of inclination of the vertical sidewalls is varied from 45° to -15° while the base wall is considered to be tilted at $0^\circ, 15^\circ$, and 30° to observe the heat transfer performance in terms of average Nusselt number with the variation of Rayleigh number.

Mathematical Formulation

A trapezoidal cavity of length L and height H is considered in Figure 1 having the sidewalls inclined at an angle \varnothing with the y -axis. The base wall is considered to be tilted at $\psi = 0^\circ, 15^\circ$, and

30° respectively with the horizontal x -axis. The trapezoid is symmetrical about the vertical central axis and has equal length and height ($L = H$). The fluid is assumed to be incompressible, Newtonian and laminar. The Boussinesq approximation is adopted to account for the variations of temperature as a function of density and to couple in this way the temperature field to the flow field. The dissipation effect due to the viscous term is neglected and no heat generation is considered. Then the governing equations for steady natural convection using conservation of mass, momentum and energy can be written in the dimensionless form as follows:

$$\frac{\partial U}{\partial X} + \frac{\partial V}{\partial Y} = 0 \tag{1}$$

$$U \frac{\partial U}{\partial X} + V \frac{\partial U}{\partial Y} = -\frac{\partial P}{\partial X} + Pr \left(\frac{\partial^2 U}{\partial X^2} + \frac{\partial^2 U}{\partial Y^2} \right) + (Ra Pr \sin \Psi) \theta \tag{2}$$

$$U \frac{\partial V}{\partial X} + V \frac{\partial V}{\partial Y} = -\frac{\partial P}{\partial Y} + Pr \left(\frac{\partial^2 V}{\partial X^2} + \frac{\partial^2 V}{\partial Y^2} \right) + (Ra Pr \cos \Psi) \theta \tag{3}$$

$$U \frac{\partial \theta}{\partial X} + V \frac{\partial \theta}{\partial Y} = \frac{\partial^2 \theta}{\partial X^2} + \frac{\partial^2 \theta}{\partial Y^2} \tag{4}$$

where U and V are the velocity components in the X and Y directions respectively, θ is the temperature, P is the pressure, Ra and Pr are the Rayleigh number and Prandtl number respectively.

Eqns. (1) - (4) are normalized using the following dimensionless scales:

$$X = \frac{x}{L}, Y = \frac{y}{L}, U = \frac{uL}{\alpha}, V = \frac{vL}{\alpha}, P = \frac{pL^2}{\rho\alpha^2}, \theta = \frac{T - T_c}{\Delta T}$$

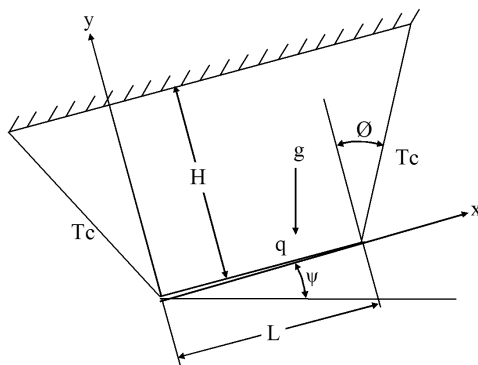


Figure 1. Schematic diagram of the physical system

$$\Delta T = \frac{qL}{k}, Ra = \frac{g\beta qL^4}{\alpha\nu k} \text{ and } Pr = \frac{\nu}{\alpha}$$

Here ρ , β , ν , α and g are the fluid density, coefficient of volumetric expansion, kinematic viscosity, thermal diffusivity, and gravitational acceleration, respectively. The corresponding boundary conditions for the above problem are given by:

$$\text{All walls: } U = V = 0, \text{ Top wall: } \frac{\partial\theta}{\partial Y} = 0, \text{ Inclined sidewalls: } \theta = 0, \text{ Bottom wall: } \frac{\partial\theta}{\partial Y} = -1 \quad (5)$$

The average Nusselt number can be written as,

$$Nu = \int_0^1 \frac{1}{\theta_s(X)} dX \quad (6)$$

where $\theta_s(X)$ is the local dimensionless temperature of the heated surface.

Numerical Procedure

The governing equations are solved numerically using a Galerkin weighted residual method of finite element formulation. A mixed finite element (FE) model is implemented with two types of triangular Lagrange elements: an element with linear velocity and pressure interpolations for the continuity and momentum equations and an element with a quadratic basis velocity and temperature interpolations for the energy equation. A stationary nonlinear solver is used together with Direct (UMFPACK) linear system solver. The relative tolerance for the error criteria is considered to be 10^{-6} . As the dependent variables vary greatly in magnitude, manual scaling of the dependent variables is used to improve numerical convergence. The manual scaling values are kept constant and selected in such a way that the magnitudes of the scaled degrees of freedom become one. The nonlinear equations are solved iteratively using Broyden's method with an LU-decomposition preconditioner, always starting from a solution for a nearby Rayleigh number. The numerical simulations are performed by varying the number of elements in order to increase the accuracy and efficiency for the solutions. Non-uniform grids of triangular element are employed with denser

grids clustering in regions near the heat sources and the enclosed walls. It may be noted that a similar finite element method has been used to solve fluid flow and heat transfer problems in recent investigations by Lo *et al.* (2005); Roy and Basak (2005) and Asaithambi (2003).

Grid Sensitivity Check

Test for the accuracy of grid sensitivity is examined for the arrangements of five different non-uniform grid systems with the following number of elements within the trapezoidal enclosure: 3,376; 4,930; 6,006; 9,006 and 11,232. The results are shown in Table 1. From these comparisons, it is suggested that 9006 non-uniform elements are sufficient to produce accurate result.

Code Validation

Since the validation against experimental data is not possible in the present case, the computational code is validated with the results obtained for natural convection flows in a trapezoidal enclosure as mentioned by Natarajan *et al.* (2008). The comparison of the result is shown in Figure 2 and it has been observed that the present numerical solution is almost in complete agreement with the aforementioned one in terms of the isotherm plot. Therefore, it can be decided that the current code can be used to predict the flow and thermal field for the present problem accurately. However, almost similar experimental results for square straight enclosure with discrete bottom heating obtained by Corvaro and Paroncini (2008) are compared by the present code and reported in Table 2. The agreement is found to be excellent which validates the present computations and lend us confidence for the use of the present code.

Results and Discussion

In the present research work, the working fluid inside the trapezoidal cavity is chosen as air with Prandtl number, $Pr = 0.7$. The sidewall inclination angles (θ) are taken as 45° , 30° , 15° , 0° , and -15° . So the top adiabatic wall of the trapezoid gets shorter and for $\theta = 0^\circ$, the trapezoid becomes

square in shape and finally it tends to be a triangle. The Rayleigh number (Ra) is varied from 10^3 to 10^6 and the tilt angle of the base wall (ψ) is varied from 0° to 30° . Flow and temperature fields are presented in terms of streamline and isotherm contours respectively. Effects of the Rayleigh number, the inclination angle of the sidewalls and the tilt angle of the base wall on the heat and fluid flow phenomenon are observed. Later, heat transfer performance is examined in terms of average Nusselt number (Nu) to predict the characteristics of natural convection under different geometric conditions.

Effects of Rayleigh Number on Heat and Fluid Flow Field

The evolution of flow and thermal fields within the trapezoidal enclosure for $Ra = 10^3, 10^5$, and 10^6 and $\theta = 45^\circ, 30^\circ, 15^\circ, 0^\circ$, and -15° is presented in Figures 3 and 4 when the base wall is considered horizontal ($\psi = 0^\circ$). Due to the symmetrical boundary conditions of the inclined sidewalls, the flow and temperature fields are symmetrical about the vertical central axis of the enclosure. As expected, hot fluid rises up from the central region as a result of buoyancy forces,

Table 1. Comparison of the results for various grid dimensions at $Ra = 10^6, \theta = 45^\circ$ and $\psi = 0^\circ$

Elements	3,376	4,930	6,006	9,006	11,232
Nu	5.900	5.884	5.876	5.866	5.865

Table 2. Comparison between the experimental and numerical average Nusselt number for discrete isothermal heat source size = 0.2, $\theta = 0^\circ$ and $\psi = 0^\circ$

Ra	Experimental Data Corvaro and Paroncini (2008)	Numerical Data Present code	Error (%)
7.56×10^4	4.80	5.31	-10.63
1.38×10^5	5.86	6.07	-3.60
1.71×10^5	6.30	6.37	-1.11
1.98×10^5	6.45	6.58	-2.01
2.32×10^5	6.65	6.82	-2.56
2.50×10^5	6.81	6.94	-1.91

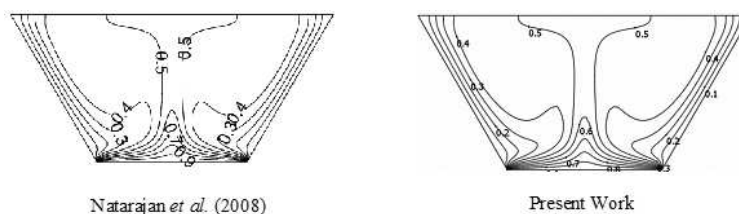


Figure 2. Comparison of the isotherm plots with Natarajan *et al.* (2008) at $Ra = 10^5, Pr = 0.7, \theta = 30^\circ$ and $\psi = 0^\circ$

after that owing to the cold inclined walls, flows down along the walls forming two symmetric rolls (Figure 3) with clockwise and anticlockwise rotations inside the cavity. At $Ra = 10^3$, viscous forces are more dominant than the buoyancy forces and hence, heat transfer is essentially diffusion dominated and the shape of the streamline tends to follow the geometry of the enclosure. For $Ra = 10^5$ and 10^6 , it is interesting to observe that the stream function contours near the walls tend to have neck formation due to stronger circulation at higher Rayleigh number which contrasts the flow pattern for $Ra = 10^3$. The core of the circulating rolls moves upward with the increase of Ra indicating significant increase of the intensity of convection.

For $Ra = 10^3$ as can be expected, heat transfer characteristics are essentially diffusion dominant as further indicated by the isotherm patterns shown in Figures 3, 5, and 7. As a representative case, for $\varnothing = 45^\circ$ and $\psi = 0^\circ$ (Figure 3), during diffusion dominant heat transfer, the temperature contours with $\theta \leq 0.14$ occur symmetrically near the side walls of the enclosure. The other isotherm lines with $\theta > 0.14$ are smooth curves symmetric with respect to the vertical symmetric line. The distortion of the isotherm field increases with enhanced buoyancy as Ra increases, where the heat transfer becomes increasingly advection dominant. The circulations are greater near the center and least at the wall due to no-slip boundary condition. Due to the initiation of advection, the isotherms are significantly distorted and pushed near the sidewalls for higher Ra . Moreover, as a representative case, Figure 3 shows for $\varnothing = 45^\circ$ isotherm with $\theta = 0.06$ which breaks into two symmetric contour lines at $Ra = 10^6$. Consequently at $Ra = 10^6$, the temperature gradients near the bottom and the sidewalls tend to be significant to develop the thermal boundary layer. Due to greater circulation at the top half of the enclosure, there are small gradients in temperature at the central regime whereas a large stratification zone of temperature is found at the vertical symmetry line due to the stagnation of flow. Formation of thermal boundary layer is observed partially for $Ra = 10^3$ and almost throughout the enclosure

for $Ra = 10^5$ and 10^6 . As the nonlinearity of the isotherms increases with the increase of Ra (10^5 and 10^6), a mushroom profile is observed in the Figures 3, 5, and 7.

Effects of Inclination Angle of the Side Walls on Heat and Fluid Flow Field

The development of the flow and thermal fields in the cavity with increasing inclination angle of the sidewalls are shown in Figures 3 - 8. For horizontal base wall (Figure 4), at $Ra = 10^3$, 10^5 and 10^6 , as the inclination angle, \varnothing , decreases the streamline contour tends to take circular shape indicating weaker flow. The circulation strength of the trapezoid with $\varnothing = -15^\circ$ is observed to be the most and it exceeds the intensity of the square cavity. During diffusion dominant heat transfer, for $Ra = 10^3$ and $\varnothing = 45^\circ$, (Figure 3) temperature contours with $\theta \geq 0.16$ are nearly smooth curves which span from the middle bottom of the enclosure and they are generally symmetric with respect to the vertical center line. With the decrease of \varnothing , the sidewalls continue to come closer to the heat flux boundary and as a result, for $\varnothing = -15^\circ$ (Figure 3), the similar pattern of isotherm is observed at $\theta \geq 0.02$ and no isothermal line is found to be broken into symmetry indicating better heat transfer performance. At $Ra = 10^6$, for advection dominant heat transfer regime, the effect of inclination angle is less significant on heat transfer compared to the diffusion dominant regime as the isotherm patterns remains almost identical.

Effects of Tilt Angle of the Base Wall on Heat and Fluid Flow Field

The base wall of the trapezoidal enclosure is considered to be tilted at an angle $\psi = 0^\circ$, 15° , and 30° to investigate fluid flow and heat transfer characteristics. The flow and thermal fields in the cavity with different tilt angles are shown in Figures 3 to 8. At Figure 4, it is observed that for the horizontal cavity ($\psi = 0^\circ$), where the buoyancy force is acting only in y direction, two recirculation cells are formed and the streamline plot is symmetric about the vertical midline owing to the symmetry of the problem geometry

and the boundary conditions. For the inclined enclosures (Figures 5 - 8) this symmetry is completely destroyed due to the buoyancy force components acting in both X and Y directions. The effect of the base wall tilting is clearly visible on the flow patterns for all cases. Though similar effect is observed on isotherm contours inside the cavity for higher Ra, the contours remain unaltered for $Ra = 10^3$ at diffusion dominant regime. From Figure 8 for $\psi = 30^\circ$, in

case of square cavity ($\varnothing = 0^\circ$), it is observed that the left recirculation vortex becomes dominating in the enclosure, the right vortex is squeezed thinner and ultimately forms minor vortices or local eddies at the corners. This circulation inside the cavity is greater near the center and least at the wall due to no slip boundary condition. Eddy formation is observed for the trapezoid with $\varnothing = -15^\circ$ while $\psi = 15^\circ$ (Figure 6) and no eddy is created in the square cavity

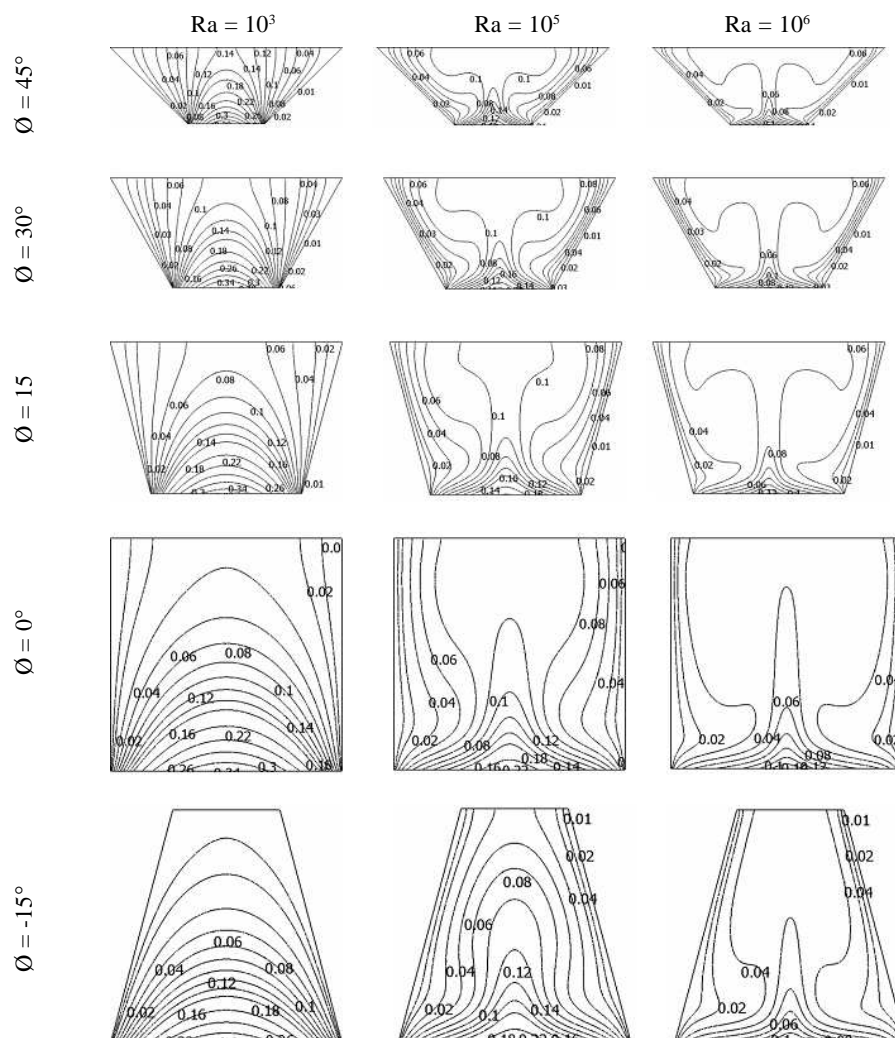


Figure 3. Isotherm plots in the trapezoidal cavity for different Rayleigh numbers and sidewall inclination angles at base wall tilt angle, $\psi = 0^\circ$

($\varnothing = 0^\circ$) with this base wall tilt condition. Interestingly, for larger sidewall inclination angles ($\varnothing = 15^\circ, 30^\circ, \text{ and } 45^\circ$), no eddy formation is observed inside the enclosure indicating less effect of base wall tilting. The isotherms are also adjusted according to the change in the flow fields and pushed towards the lower part of the right inclined sidewall indicating the presence of a large temperature gradient there.

Heat Transfer Characteristics

Finally, the present investigation concentrates on the influence of the sidewall inclination angle (\varnothing) and base wall tilt angle (ψ) for the variations of average Nusselt number of the heated wall with the Rayleigh number. In order to observe the results, the variations of average Nusselt number with $Ra = 10^3$ to 10^6 and $\varnothing = -15^\circ, 0^\circ, 15^\circ$,

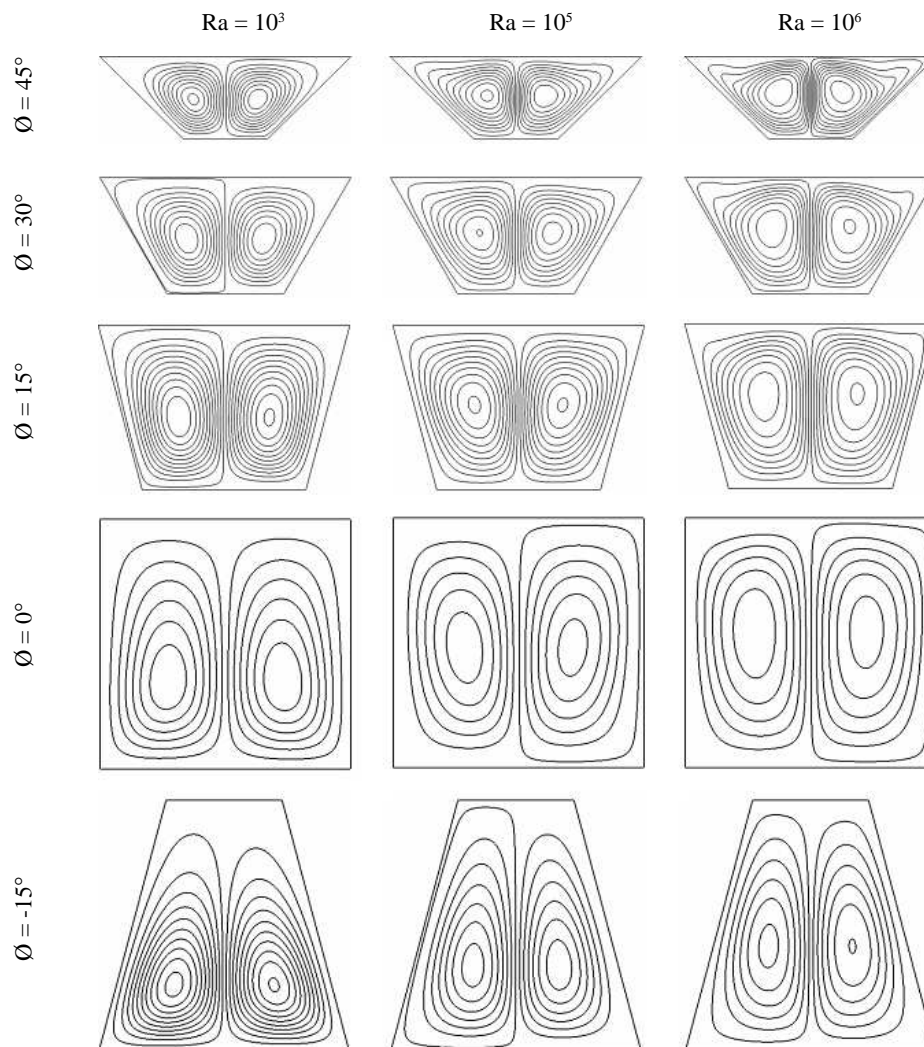


Figure 4. Streamline plots in the trapezoidal cavity for different Rayleigh numbers and sidewall inclination angles at base wall tilt angle, $\psi = 0^\circ$

30°, and 45° are plotted for base wall tilt angle $\psi = 0^\circ, 15^\circ$ and 30° in Figures 9(a-c) respectively. Figure 9(a) indicates that the average Nusselt number remains invariant up to a certain value of Ra and then increases rapidly with increasing Ra. At lower Ra, the curves maintain a flat trend indicating little change in Nu and the least slope is found for the least side wall inclination angle which indicates low temperature gradients.

Diffusion dominant heat transfer is demonstrated at $Ra = 10^3$ and significant effect of advection is initiated from $Ra = 10^4$. For higher value of sidewall inclination angle, advection is found to be initiated earlier.

At the diffusion dominant regime, the difference between the values of Nu for different sidewall inclination angles is significant whereas at $Ra = 10^6$, for the advection dominant regime

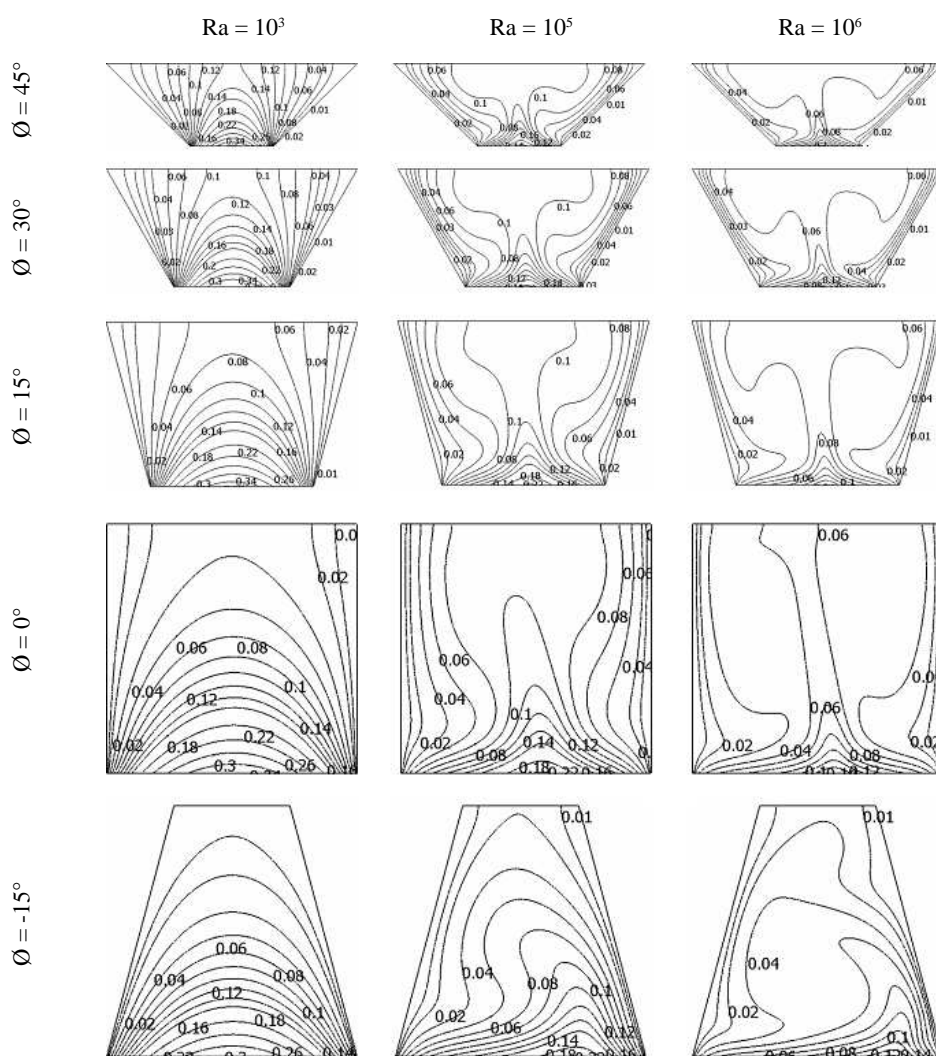


Figure 5. Isotherm plots in the trapezoidal cavity for different Rayleigh numbers and sidewall inclination angles at base wall tilt angle, $\psi = 15^\circ$

the difference of the values of Nu is found to be reduced (Figure 9(a)). The Nusselt number is the highest for the lowest inclination angle. It can be decided that as the sidewall inclination angles decrease the trapezoid tends to get rectangular geometry and the constant temperature sidewalls acting as the heat sinks come closer to the heat source resulting improved heat transfer inside the cavity.

From Figures 9(a-c), it is evident that there

is no effect of base wall tilt angle on average Nusselt number at lower Ra . But at $Ra > 10^4$, when the heat transfer mechanism is essentially dominated by advection, effect of ψ increases on the heat transfer characteristics. However, trapezoidal enclosures with positive \emptyset are less affected with the change in ψ compared to the square cavity and the trapezoidal cavity with negative \emptyset . Figure 9(b) indicates that at $Ra = 10^5$ to 10^6 for $\psi = 30^\circ$, change in the sidewall inclina-

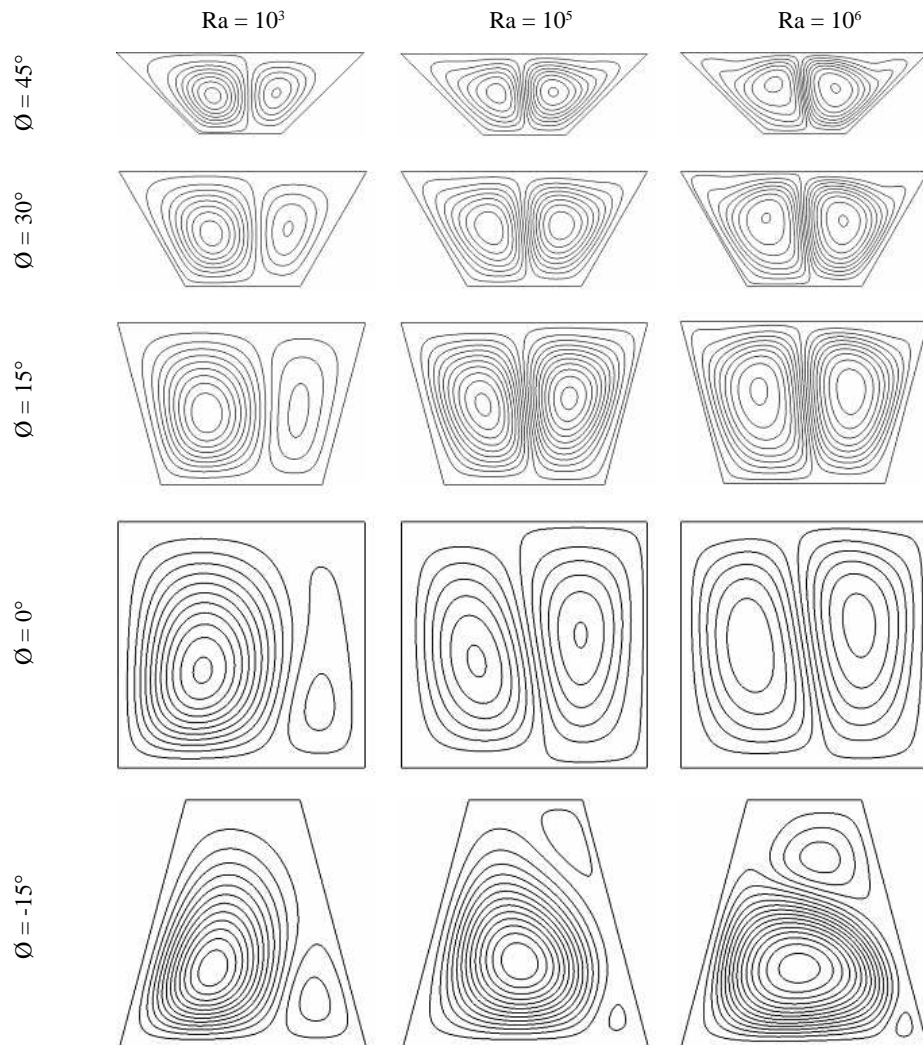


Figure 6. Streamline plots in the trapezoidal cavity for different Rayleigh numbers and sidewall inclination angles at base wall tilt angle, $\psi = 15^\circ$

tion angle after $\varnothing = 15^\circ$ does not influence the heat transfer performance so much while the trapezoid with $\varnothing = -15^\circ$ shows the highest value of Nu and the square cavity shows the lowest value. Trapezoidal enclosures with positive value of \varnothing remain in between without any significant change in the heat transfer performance. Therefore, $Ra = 10^5$ can be considered as a critical limit for the current problem. Finally, it is observed that the overall heat transfer performance dete-

riorate in terms of Nu with the increase of the base wall tilt angle.

Conclusions

Natural convection in a two-dimensional trapezoidal enclosure, where the top wall is considered adiabatic, two inclined sidewalls are maintained at constant low temperature and an isoflux heat source is applied on the bottom

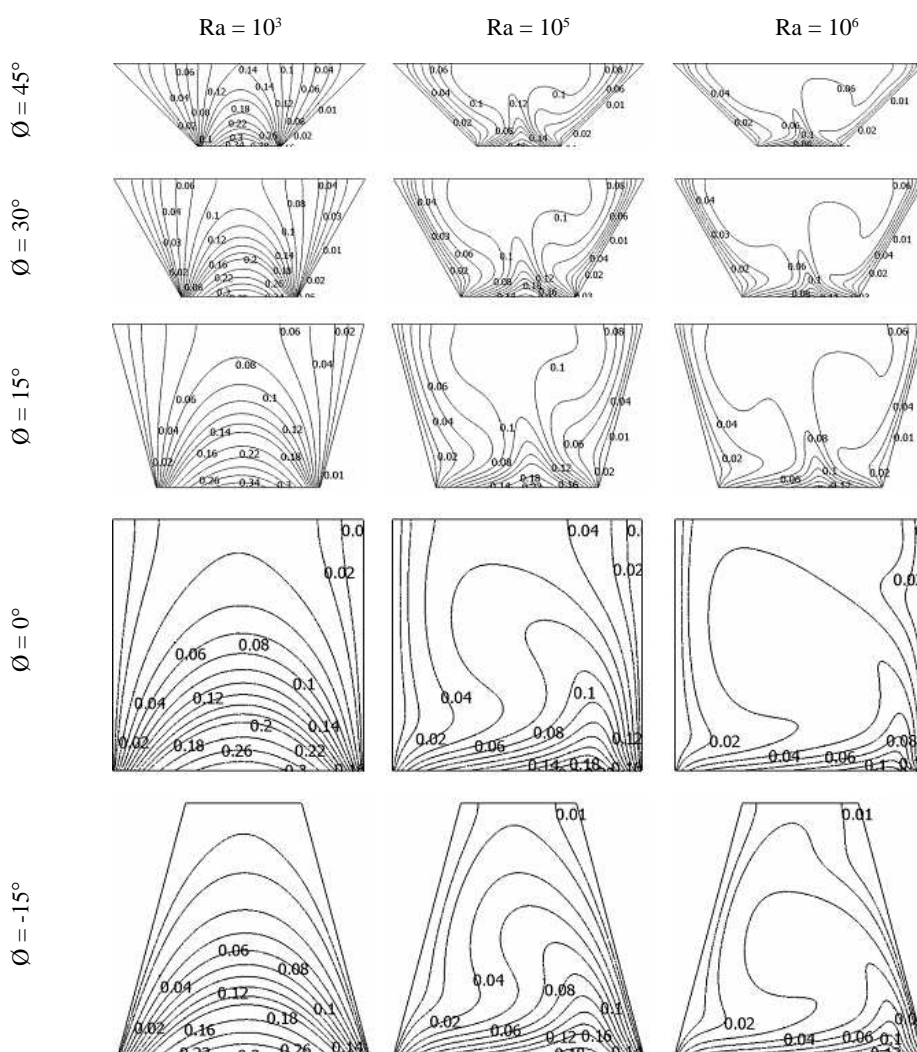


Figure 7. Isotherm plots in the trapezoidal cavity for different Rayleigh numbers and sidewall inclination angles at base wall tilt angle, $\psi = 30^\circ$

wall has been analyzed numerically using finite element method under different base wall tilt conditions. The main parameters of interest are the Rayleigh number (Ra), the sidewall inclination angle (\emptyset), and the base wall tilt angle (ψ). It has been observed that the diffusion dominant heat transfer modes are found for $Ra \leq 10^3$ and the circulation is so weak that the viscous forces are dominant over the buoyancy forces. At the advection dominant regime, for $Ra \geq 10^5$ the

compression of isotherms and the formation of thermal boundary layer increase due to increased circulation intensity. The average Nusselt number is higher for lower sidewall inclination angle indicating higher heat transfer. At advection dominant regime for higher Rayleigh number, the variation of average Nusselt number tends to be significantly reduced with the change of the sidewall inclination angle.

Heat transfer performance in terms of

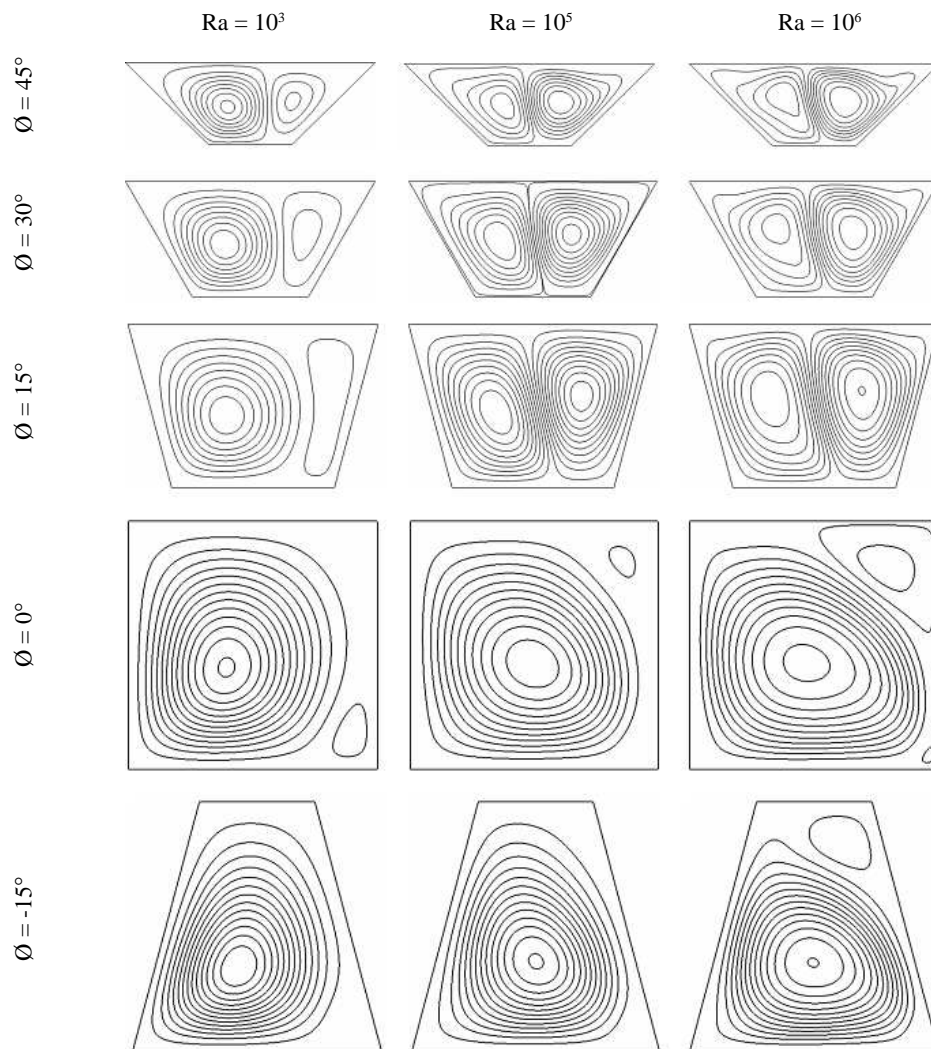


Figure 8. Streamline plots in the trapezoidal cavity for different Rayleigh numbers and sidewall inclination angles at base wall tilt angle, $\psi = 30^\circ$

average Nusselt number inside the cavity increases as the cold sidewalls acting as the heat sinks come closer to the hot bottom heat source. Effects of sidewall inclination angle decrease with the increase of base wall tilt angle at higher Rayleigh number. At the diffusion dominant regime, for $Ra = 10^3$ no significant influence of the variation of the base wall tilt angle is observed. With the increase of the tilt angle overall heat transfer rate is found to be decreased

inside the trapezoidal enclosure at the advection dominant regime.

References

Asaithambi, A. (2003). Numerical solution of the Falkner-Skan equation using piecewise linear functions. *Applied Mathematical Computations*, 81:607-614.
 Baytas, A.C. and Pop, I. (2001). Natural convec-

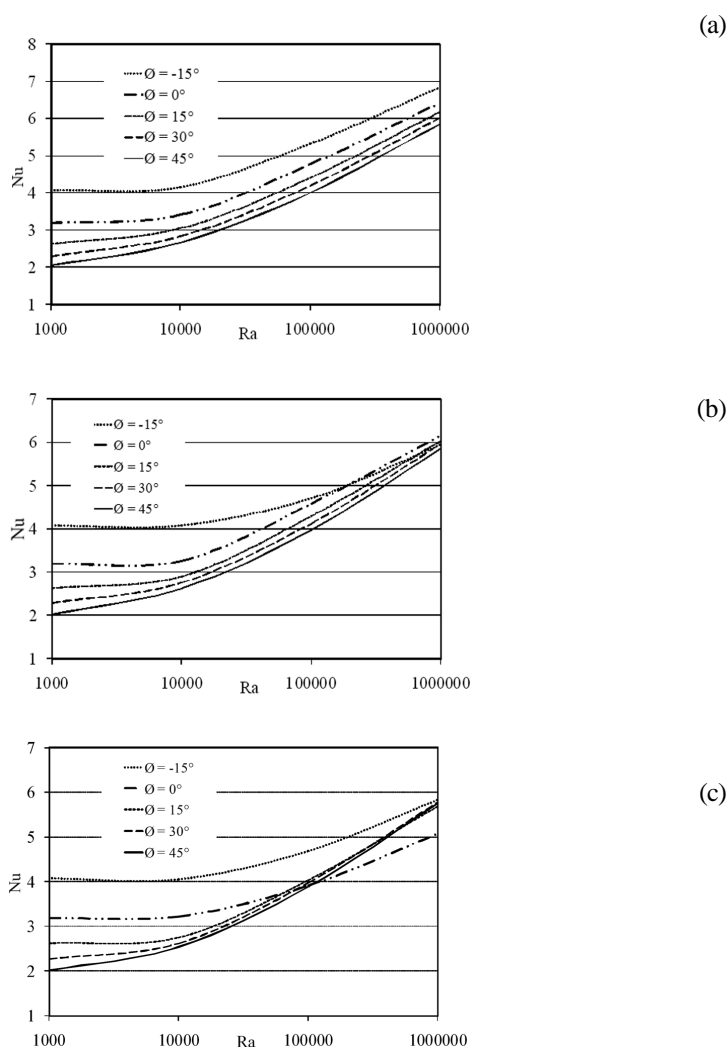


Figure 9. Variation of average Nusselt number with Rayleigh number for different inclination angles at base wall tilt angle, (a) $\psi = 0^\circ$, (b) $\psi = 15^\circ$, and (c) $\psi = 30^\circ$

- tion in a trapezoidal enclosure filled with a porous medium. *Int. J. of Engineering Science*, 39:125-134.
- Baïri, A., Laraqi, N., and García de María, J.M. (2007). Numerical and experimental study of natural convection in tilted parallelepipedic cavities for large Rayleigh numbers. *Exp. Thermal and Fluid Science*, 31:309-324.
- Bejan, A. (1984). *Convection Heat Transfer*. 1st ed. John Wiley & Sons, Inc., 494p.
- Boussaid, M., Mezenner, A., and Bouhadeh, M. (1999). Free heat and mass convection in a trapezoidal enclosure. *Int. J. Therm. Sci.*, 38:363-371.
- Corvaro, F. and Paroncini, M. (2008). A numerical and experimental analysis on the natural convection heat transfer of a small heating strip located on the floor of a square cavity. *Applied Thermal Engineering*, 28:25-35.
- Flack, R.D., Konopnicki, T.T., and Rooke, J.H. (1980). The measurement of natural convective heat transfer in triangular enclosure. *J. Heat Transfer*, 102:770-772.
- Ganzarolli, M.M. and Milanez, L.F. (1995). Natural convection in rectangular enclosures heated from below and symmetrically cooled from the sides. *Int. J. Heat and Mass Transfer*, 38:1,063-1,073.
- Iyican, L. and Bayazitoglu, Y. (1980). An analytical study of natural convective heat transfer within trapezoidal enclosure. *ASME J. Heat Transfer*, 102:640-647.
- Kumar, R.B.V. and Kumar, B. (2004). Parallel computation of natural convection in trapezoidal porous enclosures. *Mathematics and Computers in Simulation*, 65:221-229.
- Kumar, S. (2004). Natural convective heat transfer in a trapezoidal enclosure of box-type solar cooker. *Renewable Energy*, 29:211-222.
- Kuyper, R.A. and Hoogendoorn, C.J. (1995). Laminar natural convection flow in trapezoidal enclosures. *Numer. Heat Transfer, Part A*, 28: 55-67.
- Lo, D.C., Young, D.L., and Lin, Y.C. (2005). Finite-element analysis of 3D viscous flow and mixed-convection problems by the projection method. *Numer. Heat Transfer, Part A*, 48:339-358.
- McQuain, W.D., Ribbens, C.J., Wang, C.Y., and Watson, L.T. (1994). Steady viscous flow in a trapezoidal cavity. *Computers Fluids*, 23:613-626.
- Natarajan, E., Basak, T., and Roy, S. (2008). Natural convection flows in a trapezoidal enclosure with uniform and non-uniform heating of bottom wall. *Int. J. of Heat and Mass Transfer*, 51:747-756.
- Nithyadevi, N., Kandaswamy, P., and Lee, J. (2007). Natural convection in rectangular cavity with partially active side walls. *Int. J. of Heat and Mass Transfer*, 50:4,688-4697.
- Papanicolaou, E. and Belessiotis, V. (2005). Double-diffusive natural convection in an asymmetric trapezoidal enclosure: unsteady behavior in the laminar and the turbulent-flow regime. *Int. J. of Heat and Mass Transfer*, 48:191-209.
- Reddy, J.N. (1993). *An Introduction to the Finite Element Method*. 2nd ed. McGraw-Hill, NY, 896p.
- Remley, T.J., Abdel-Khalik, S.I., Jeter, S.M., Ghiaasiaan, S.M., and Dowling, M.F. (2001). Effect of non-uniform heat flux on wall friction and convection heat transfer coefficient in a trapezoidal channel. *Int. J. Heat and Mass Transfer*, 44:2,453-2,459.
- Reynolds, D.J., Jance, M.J., Behnia, M., and Morrison, G.L. (2004). An experimental and computational study of the heat loss characteristics of a trapezoidal cavity absorber. *Solar Energy*, 76:229-234.
- Roy, S. and Basak, T. (2005). Finite element analysis of natural convection flows in a square cavity with non-uniformly heated wall(s). *Int. J. Engineering Science*, 43:668-680.
- Vander Eyden, J.T., Van der Meer, TH.H., Hanjalić, K., Biezen, E., and Bruining, J. (1998). Double-diffusive natural convection in trapezoidal enclosures. *Int. J. of Heat and Mass Transfer*, 13:1,885-1,898.